

Enhancing the efficiency, productivity, stabilizing operating conditions and pollution reduction of Benghazi North power plant by solar cooling

م. عبد الحفيظ التاجوري أ.د. عوض بودلال
م. صلاح الصفراني أ.د. صلاح المشيطي

Abstract:

Benghazi North power plant is subjected to large ambient temperature and sea water temperature fluctuations throughout the year, which adversely impacts on the performance, and the generated power consequently increasing of CO₂ emission rates. Stabilising the inlet air temperature and controlling the condenser inlet cooling water temperature at the design condition enhances and maintains the performance and efficiency throughout the year. A system of a single effect water- lithium bromide absorption cycle powered by solar parabolic trough collector and for efficient operation during the non-sunny periods, an insulated thermal storage tank was introduced to store thermal energy of the working medium, and an assisting heat energy supply coming from HRSG downstream exhaust gases to make up any temperature drop inside the tank, which must not be less than 80 °C, to ensure the effectiveness of the cooling system operation.

The results of the model indicate improving the overall efficiency by 3.635% and the generated power by 12.18% reducing the emissions of greenhouse gases produced by the plant by 3.537% .The annual power output increased by 9.767 % and 7.728% for the gas turbine standalone and the combined cycle power plant respectively and the net electricity

production increases by 141,358,530kWh/yr, which can save 14,135,853\$/y .Although the capital cost is relatively high, the payback period is 1.48 years at the selling price of energy of 0.1 \$/kwh based on the average selling price of kilowatt hour of electricity in Libya in 2015.The annual solar contribution factor of the solar parabolic trough system was calculated and attained the value of 91.896 % for sunny periods.

1.Introduction:

The world's population is dramatically increased and the demand for energy is greater than ever before. Fossil fuels such as coal, oil and natural gas are the main source of energy that powers our life style and the world economy but they are not renewable sources meaning that once used they cannot be replaced.

Several gas turbines are being widely used for power generation in several countries all over the world. Obviously, many of these countries have a wide range of climatic conditions, which impact the performance of gas turbines. Problems rise when a gas turbine is used in a geographic location with hot summers. Hot inlet air results in a gas turbine's generating less power, during summer season, when the demand for electricity is at its peak point .

In such conditions, power augmentation techniques are highly desirable. Indeed, a minor increase of thermal efficiency could result in a significant amount of fuel being saved and a higher level of power being

generated. The simplest remedy to this problem is to reduce the temperature of the inlet air. Several different inlet cooling methods are currently employed in various systems [1]. The International Institute of Refrigeration (IIR) has estimated that approximately 15% of all electricity produced worldwide is used for refrigeration and air conditioning processes of various kinds [2].

1.1 Electricity in Libya

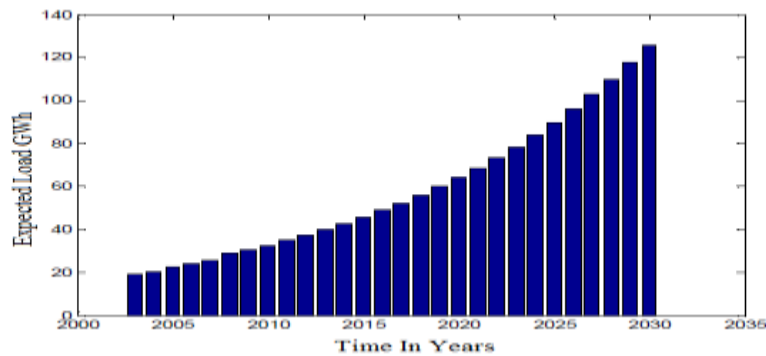


Figure1.1: Expected load demand for the next 20 years [3]

The national electric grid consists of a high voltage network of about 12,000 km, a medium voltage network of about 12,500 km and 7,000 km of low voltage network. The installed capacity is 5600 MW with a peak Load of 3650 MW, for the year 2004 Fig.1.1. In spite of that; there are many villages and remote areas located far away from these networks. Economically these areas cannot be connected to the grid, owing to its small population, and small amount of energy required. In the past these

facts dictate the use of diesel generators as a power supply. The use of diesel generators needs continuous maintenance, continuous supply of fuel. For these reasons we are pushed to look into some other sources like renewable energy. Moreover renewable energy provides clean and reliable energy sources which can be used in many applications in remote areas (electricity, water pumping, etc.). The use of renewable energies has been introduced in a wide range of applications due to its convenient use and being economically attractive in many applications. The most important renewable energy sources are solar energy, wind energy, and biomass [4].

1.2 Renewable Energy in Libya

Libya is located in the middle of North Africa with 88% of its area considered to be desert areas, the south is located in the Sahara desert where there is a high potential of solar energy which can be used to generate electricity by both solar energy conversions, photovoltaic, and thermal [4].

1.3 Recourses Estimation For Libya

The renewable energy sources estimated for Libya according to the MED-CSP scenario is shown in Table1.1.

Table1.1:Renwable enregy sources for libya[4].

Type	Potential	
Solar electricity	140,000	Twh/year
Wind electricity	15000	Twh/year
Biomass	2000	Twh/year
Total	157,000	Twh/year

Libya has a good renewable resources (solar energy and wind energy) as mentioned previously [5]. At the same time Libya has interconnection with neighboring countries as shown in Fig.1.8, which gives the merit to this country to invest in the solar and wind energy technologies (i.e. exporting the electricity produced by renewable energy). Renewable energy could be one of the 10 high growth potential sectors for the diversification of the Libyan economy ,as shown in Fig.1.3 [5].

**Figure1.2: Interconnection with Neighboring Countries [5]**

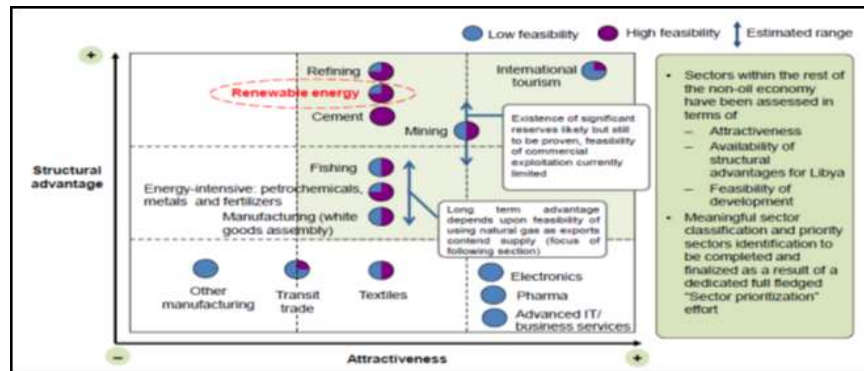


Figure1.3: Sectors for the diversification of the Libyan economy [5]

The growing demand for electrical power and serious restrictions on thermal pollution has increased the need for developing more efficient power generation systems. Any variation in the ambient temperature will affect the exhaust temperature of the compressor, the internal temperature of the turbine, the mass flow, the specific work, the specific consumption and the output power. One of the most efficient ways, to improve a gas turbine performance, especially those situated in remote hot climate conditions, is to combine it with an absorption refrigeration cycle. The waste heat of the gas turbine is used alone or integrated with solar energy to operate an absorption refrigeration unit whose cooling effect reduces air temperature at inlet to the compressor and condenser inlet cooling water temperature . This reduction in the temperature causes an increase of air density, an increase of mass flow

through the turbine, and decrease the amount of work required to drive the compressor, and therefore, an increase of overall thermal efficiency of the plant with a constant output power, independent of ambient air conditions.

Due to the limitations of the second law of thermodynamics, almost any energy conversion process is inefficient, involving loss of the energy being converted. Lawrence Livermore National Laboratory showed that, in 2016, 66.4% of total useful energy is rejected as waste energy [6]. Therefore, developing new technologies that benefit from that waste energy is essential, not just economically, but also environmentally. Most of the increase in the carbon dioxide emissions is caused by the burning of fossil fuels, which are used to generate 90% of the world's electrical energy. Many traditional fossil-fuel fired power plants have efficiencies in the range of 30 to 40 percent, but NGCC power plants are able to meet efficiencies of 50 to 60 percent [7]. The plant also loses energy through the flue gas exhaust because the gas exits to the atmosphere from the stack at a temperature higher than ambient (~80-150°C). The interest in the intake air cooling techniques for gas turbines has augmented in the last years, due the increasing requirement for power to a low specific investment cost [8]. In gas turbines since the combustion air is taken directly from the environment, their performance is

strongly affected by weather conditions .Power rating can drop by as much as 20 to 30%, with respect to international standard organization (ISO) design conditions, when ambient temperature reaches, 35 to 45°C[9]. During the last decades there has been continuous development of combined cycle power plants due to their increased efficiency and their low emissions efficiencies are very wide ranging depending on the lay-out and size of the installation and vary from about 40-56% for large new natural gas [10]. The major operating parameters which influence the combined cycle performance are: Turbine inlet temperature, Compressor pressure ratio, Ambient Temperature, Humidity, Fuels, Pressure level [11], and Condenser Inlet Cooling water Temperature[12]. Waiel Kamal, etal.[13]investigated the effect of ambient temperature and relative humidity on gas turbine power output and thermal efficiency and concluded that when the gas turbine is operated at ambient condition of relatively low temperature of 24°C and RH of 60%, there is a potential decrease of power output by about 6.3%, accompanied by a 1.8% drop in thermal efficiency and a 1.8% increase in specific fuel consumption when compared to the performance at ISO standard condition. Operating at high ambient temperature of 35°C and RH 60% when compared to ISO standard conditions, the potential power output of gas turbine decrease by about 13.65%,

accompanied by a 4.7% drop in thermal efficiency and a 4.7% increase in specific fuel consumption. When the relative humidity of the ambient air increases by 10%, the power output decrease by 0.21%, accompanied by a 0.21% drop in thermal efficiency and a 0.21% increase in specific fuel consumption. . Kamal et al. [14] discussed the feasibility of turbine inlet air cooling in Malaysia climate using mechanical chillers. They claimed that this modification is effective for power augmentation in Malaysia by 27.5% to 32.11%. Nasser and El-Kalay[15] recommended the use of a single effect water-lithium bromide absorption chiller system in Bahrain for cooling intake air of gas turbine, which is capable of increasing power output by 20% in summer. Lowering air temperature by 10 °C at 40 °C ambient condition leads to increase power by 10 %.

2. The integrated solar combined cycle

Integrating solar energy with traditional fossil fuel-fired power generation systems has become an effective way to further reduce the use of fossil fuel, improve the thermal performance of the traditional power generation system and exploit solar energy. The integrated solar combined cycle (ISCC) system was initially proposed by Johansson TB et al. [16] in the early 1990s. Solar energy was coupled with the traditional gas turbine combined

cycle (GTCC) system. It has been proven that the ISCC system can improve solar photoelectric efficiency, save the investment cost and reduce the fossil fuel consumption by integrating the solar energy [17,18]. Now the ISCC system has been applied and demonstrated around the world and is developing larger capacity and higher efficiency [18]. The thermodynamic performance of the first ISCC system built in Angola was analyzed by Omar Behar et al. [19]. The study showed that the ISCC system output power increased by 17% and the thermal cycle efficiency increased by 16.5% compared with the traditional GTCC system. M.J. Montesand Rovira [20] designed an ISCC system with the direct steam generation system (DSG) and compared it with the ISCC system with the heat transfer fluid (HTF). They concluded that the DSG technology had advantages in thermodynamic and economic performances.

Antonio Rovira [21] et al. studied the performances of integrating the solar energy into different boiler heating surfaces of the combined cycle system with DSG. The results showed that the integration of high-pressure heating surfaces had higher thermal efficiency than the integration of low-pressure heating surfaces and the single integration with the high-pressure evaporator had advantages in both the thermodynamic performance and cost. A.Baghernejad and M.

Yaghoubi [22] analyzed the exergy economic performance and sensitivity of the ISCC system with HTF trough solar technology and obtained a series of system optimization measures.

A. Baghernejad, M. Yaghoubi [23] and G.C. Bakos, D. Parsa[24] have made some economic performance analyses of solar energy trough technology integrated with the Rankine cycle. They analyzed the process of exergy loss and revealed the relationships between the cost of electricity and integration modes.

Yuanyuan Li [25,26] proposed a novel two stage ISCC system. The results showed that the system had better thermodynamic performance. The simulation results from Popov [27] showed that with enough direct normal irradiance (DNI), for single-pressure or dual-pressure HRSG, the higher the pressure of the solar energy integration section was, the greater the energy level of the solar energy was, and the higher the thermoelectric conversion efficiency was. The Iranian Chababar power station adopted the Li-Br absorption refrigeration technology, generating power of more than 14,000 W·h per year, an increase of 11.3% in output power and an internal rate of return of 23.4%. China's Shenzhen Jingang power plant also uses the Li-Br absorption refrigeration technology, so that the PG6541B gas turbine inlet temperature can be reduced from 31 °C to 17 °C. Popov [28]

proposed and compared two ISCC layouts with inlet temperature cooling, and analyzed its thermodynamic performance at design point and its cost advantages. The research results showed that a system with an absorption refrigerator has a lower levelized cost of electricity than the traditional ISCC system. Liqiang Duan et.al. [29] presented a novel ISCC system, which use the solar thermal energy integrated into the chiller for cooling the gas turbine inlet temperature and the HRSG for increasing the system power output simultaneously. Based on the changes of the environmental temperature and DNI, the new system preferentially integrates solar energy into the Li-Br absorption refrigeration system. When the gas turbine inlet temperature drops to 5 °C, then the redundant collector mirrors are integrated into the HPB section of the HRSG and compared it with the traditional ISCC system use the DSG technology with a trough parabolic field. The trough solar collector system is intergraded into the HPB section of the HRSG using the DSG technology. Through the performance calculations of a typical summer's day and atypical year, both the thermodynamic and economic advantages of the new system are deeply analyzed. The new system has higher daily and annual system thermal efficiencies (52.90% and 57.00%, respectively), higher daily and annual solar photoelectric efficiencies (31.10% and 22.31%, respectively) than

the traditional ISCC system. The solar energy levelized cost of electricity of the new ISCC system is 0.181 \$/kW·h, which is 0.061 \$/kW·h lower than that of the traditional ISCC system. .Also they concluded that the new system has high solar heat energy utilization, because the benefit of the solar energy integrated with the absorption refrigeration is greater than with the HRSG, so the solar radiation energy preferentially integrates with the Li-Br absorption refrigeration system and then integrates with the HRSG, and the absorption refrigeration can make full use of solar energy, The solar energy utilization hours of the new system are longer throughout a year, and the solar energy can be used as much as possible, which greatly reduces the average cost of the heat collection mirror, and the Li-Br absorption refrigerator has the advantages of a simple structure, fewer moving parts, a wider range of cooling and good environmental performance. and is more suitable for the gas turbine inlet air cooling which requires a larger cooling capacity. Ahmed Ali[30] concluded that the absorption chillers are promising when integrating them with power plants in dry, hot areas and recorded that The installed chillers cover the maximum cooling load demand of 4170 TR and is capable of adding 34964 KW to the net power output of a combined cycle with rated power of 267878 KW in the solar times. While 37999 KW can be gained

using a 50522 m² solar field to produce the heating fluid required to run the absorption chillers and the CO₂ emissions reduced to 0.508 kgCO₂/kwh from 0.73 kgCO₂/kwh with no air cooling. Solar thermal cooling is found more suitable than solar electric cooling, notably in areas where solar energy is always available. In addition, higher capacity and better coefficient of performance (COP) could be achieved using solar hybrid cooling systems which are mostly based on absorption chiller and mainly LiBr/H₂O machine [31]. Erkinjon Matjanov[32] in his study proposed an absorption chiller to cool the gas turbine inlet air and to drive the cooling process the absorption chiller was analyzed to use three types of heat source: the gas turbine waste gases, the HRSG waste gases, the solar energy. According to results of the study, 4260 kW heat is required in absorption chiller to reduce the inlet air temperature from 45 °C down to 15 °C. To provide the absorption chiller with 4260 kW heat of solar energy, 28 pcs parabolic trough collectors with total net aperture area 8064 m² were required. Parabolic through collectors with 50 m length, 5.76 m gross aperture width were used while simulations.

The results of the study notified , that using the heat of gas turbine waste gases in absorption chiller is not economical profitable, because CHP efficiency is reduced down from 81.4% to 74.4% during ambient temperature 45 °C, and HRSG waste gases have

enough heat to provide cooling process in the absorption chiller, only if the temperature of HRSG waste gases is bigger than 120 °C otherwise the solar field for such purpose can be economic profitable. V.C. Okafor[33] compared the effect of using evaporative cooling system pre-cooling method, vapour compression refrigeration precooling and vapour absorption refrigeration precooling techniques for cooling gas turbine inlet air. The results show that at air temperature of 38°C, the reference system, evaporative precooling, vapour compression refrigeration and vapour absorption refrigeration precooling methods recorded Net power Outputs of 23.143MW, 25.39MW, 31.84MW and 34.90MW respectively. The Thermal Efficiency Change factor recorded by the precooling systems at an ambient temperature of 38°C is 9.71%, 37.4% and 51% respectively. Absorption refrigeration recorded the highest net output power because less parasitic work is consumed unlike in vapour compression cooling system in which more parasitic work is consumed (i.e. power required to drive the refrigeration compressor). A. Ettajuri et.al.[34] introduced a system of a single effect water- lithium bromide absorption cycle with chilled water storage tank powered by integrated solar parabolic trough collector field with HRSG waste gases and hot water thermal storage tank, to cool the intake air and the condenser inlet cooling water of Benghazi North

combined cycle Power Plant. The results of the model indicate improving the overall efficiency by 3.635% and the generated power by 12.18% reducing the emissions of greenhouse gases produced by the plant by 3.537% .The annual power output increased by 9.767 % and 7.728% for the gas turbine standalone and the combined cycle power plant respectively.Solar contribution covering the cooling load of 18.24 MW was 91.89 % while the HRSG waste gases covered 8.11 % with payback period of 1.48 year.

3.The Proposed Mathematical Model:

According to the basic principle of the CCGT, the air is compressed by the air compressor and transferred to the combustion chamber where it combines with liquid or gaseous fuel for producing high-temperature flue gas through the process of combustion. Hot gases leaving the combustion chamber expands in the turbine thereby producing output work and finally discharges to the atmosphere. The waste exhaust gas temperature from gas turbine decreases as it flows into the heat recovery steam generator(HRSG). Then the HRSG supplies a steam for the steam turbine in producing electricity. The plant model of this study is an existing power plant situated in the city of Benghazi Libya and it has been connected to the Libyan grid since 1979. The power plant

Figure 3.1: Schematic diagram of the proposed solar cooling system in Benghazi North power plant.

3.2. Benghazi Climate Data:

Benghazi is the second city in Libya has an area of 314 km² and average sun shine hours of 9.589 h/d, average clearness index is 0.572 and Terrestrial radiation in Benghazi's land is 2.33022* 10¹² Wh/year with a warm semi-arid climate. To the north of the city is the Mediterranean, and to the south the climate is desert like. Summers in Benghazi are hot and dry; winters are mild with occasional rain table3.1.

Table 3.1 Benghazi Climate Data

Benghazi Climate Data	value
Average Rain Fall mm	69
Total Radiation kWh/m ² /day	7.17
Diffused Radiation kWh/m ² /day	1.6
Beam Radiation kWh/m ² /day	5.7
Latitude angle degree	32.1°
Longitude angle degree	25.15°

Benghazi Climate Data		value
Average Rain Fall mm		69
Total Radiation kWh/m ² /day		7.17
Diffused Radiation kWh/m ² /day		1.6
Beam Radiation kWh/m ² /day		5.7
Latitude angle	degree	32.1°
Longitude angle	degree	25.15°
Average Max. air Temperature	°C	17 - 32
Average Max. sea Temperature	°C	18 - 27

4.results and discussions:

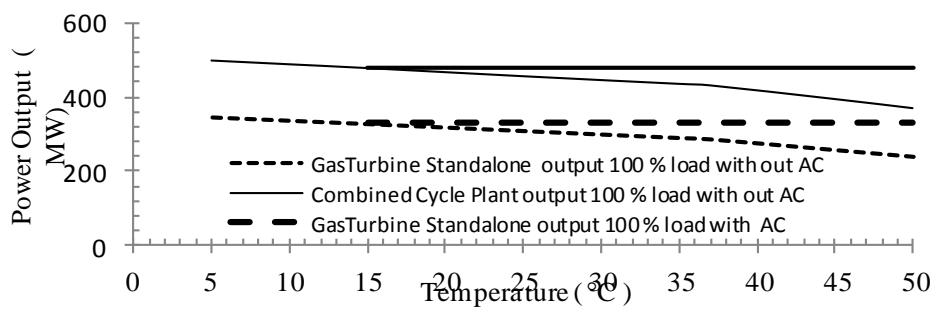


Figure 4.1: Effect Of Ambient Temperature On Benghazi North Power Plant Output.

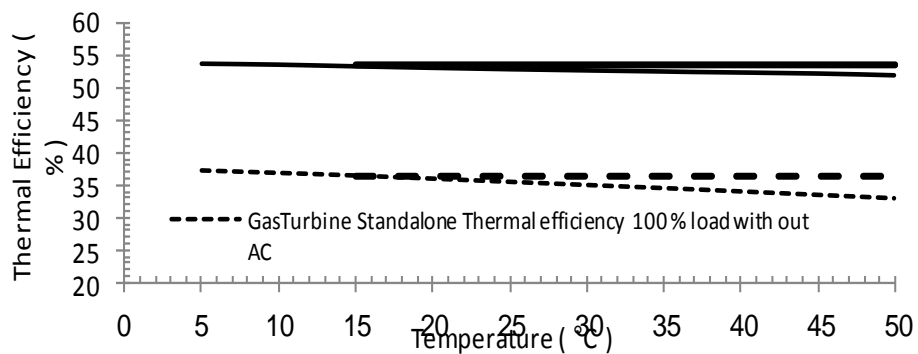


Figure 4.2 Effect Of Ambient Temperature On Benghazi North Power Plant Thermal Efficiency. **Figure 4.3: Effect Of Ambient Temperature On Benghazi North**

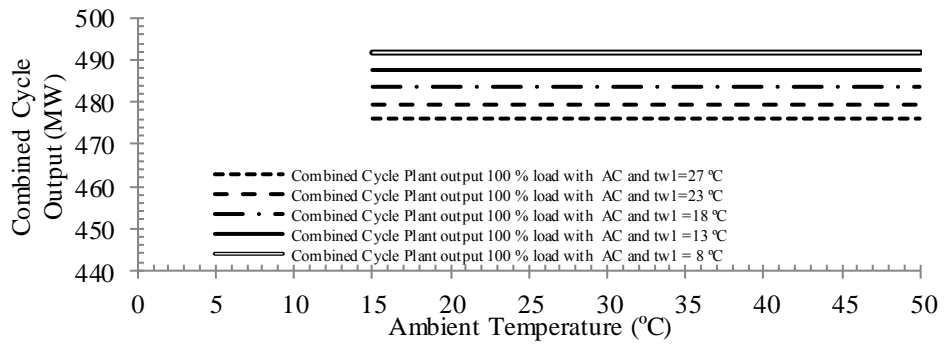
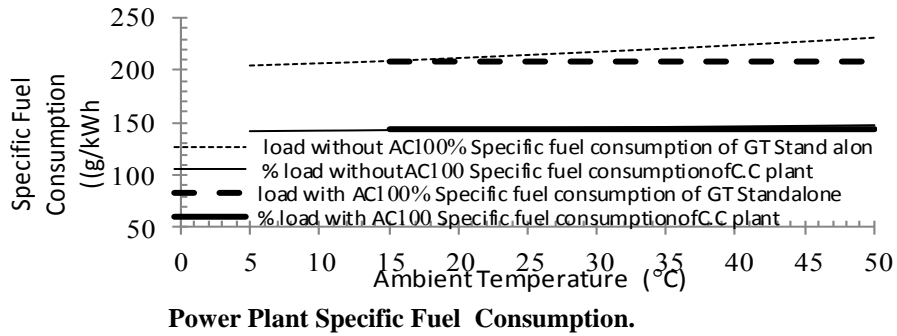
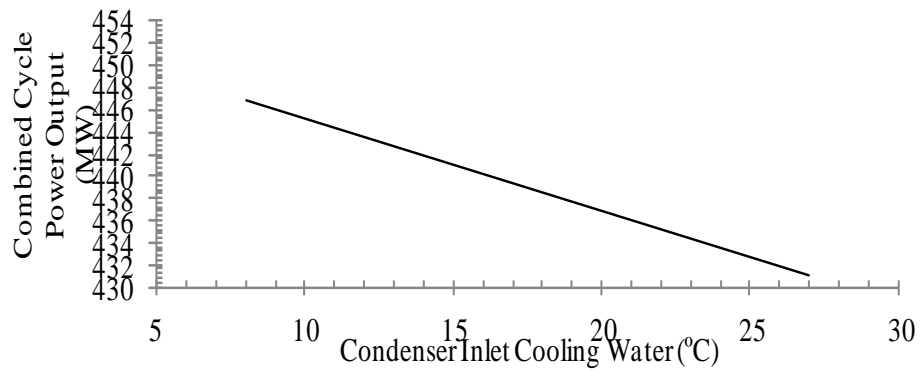


Figure 4.4: Effect of Condenser Inlet Cooling Water Variations on Benghazi North



plant Output with air cooling

Figure 4.6: Effect of Condenser Inlet Cooling Water Variations on Benghazi North plant Output without Intake Air Cooling.

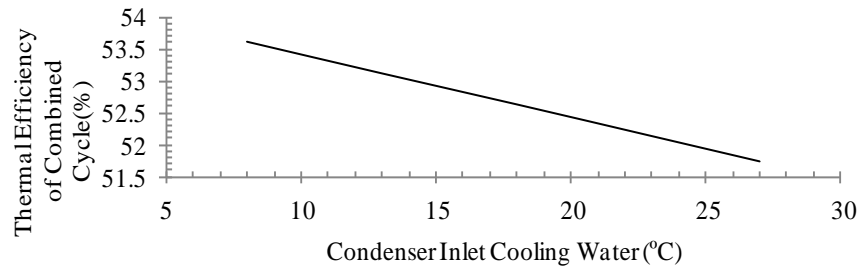


Figure 4.7: Effect of Condenser Inlet Cooling Water Variations on Benghazi North plant Thermal Efficiency without Intake Air Cooling.

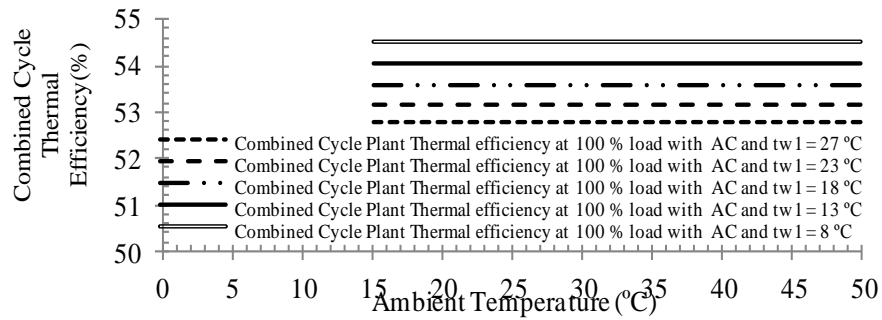


Figure 4.5: Effect of Condenser Inlet Cooling Water Variations on Benghazi North plant Thermal Efficiency with air cooling .

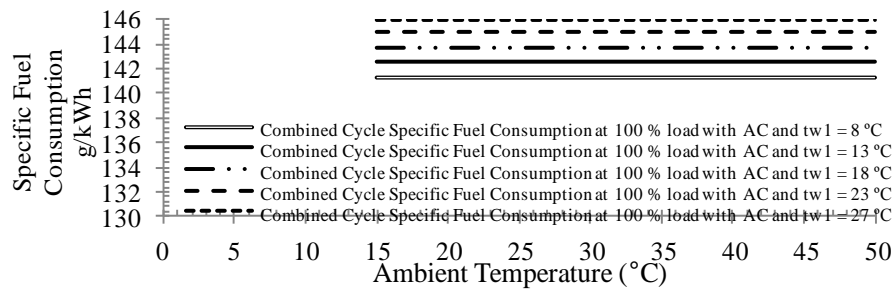


Figure 4.8 Effect of Condenser Inlet Cooling Water Variations on Benghazi North plant Specific Fuel Consumption with Intake Air Cooling .

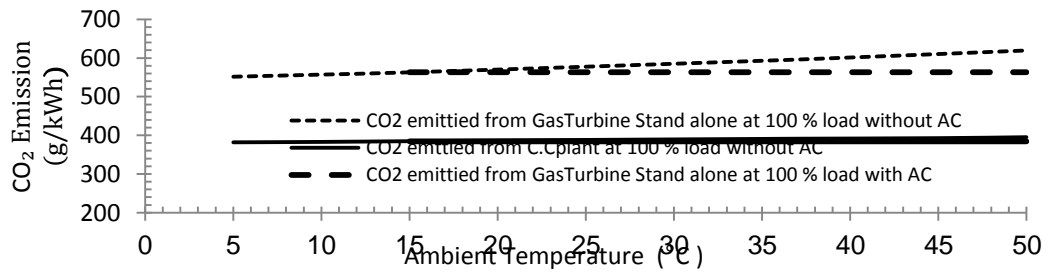


Figure 4.9: Effect Of Ambient Temperature On Benghazi North Power Plant CO₂ Emission.

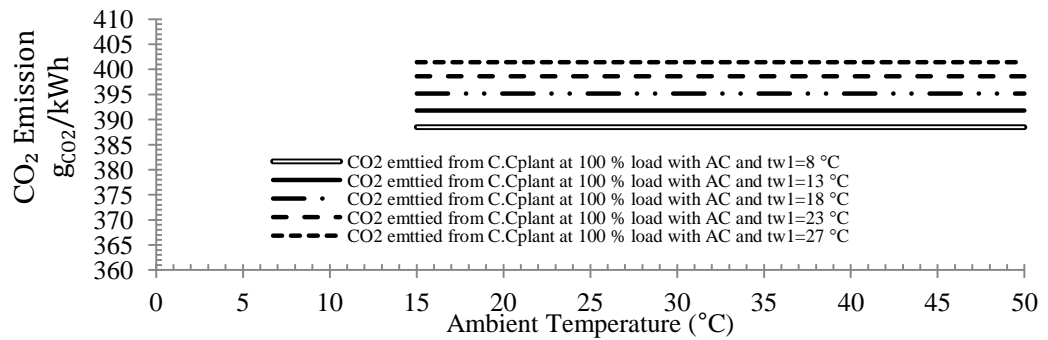


Figure 4.10: Effect of Condenser Inlet Cooling Water Variations on Benghazi North plant with Intake Air cooling CO₂ Emission.

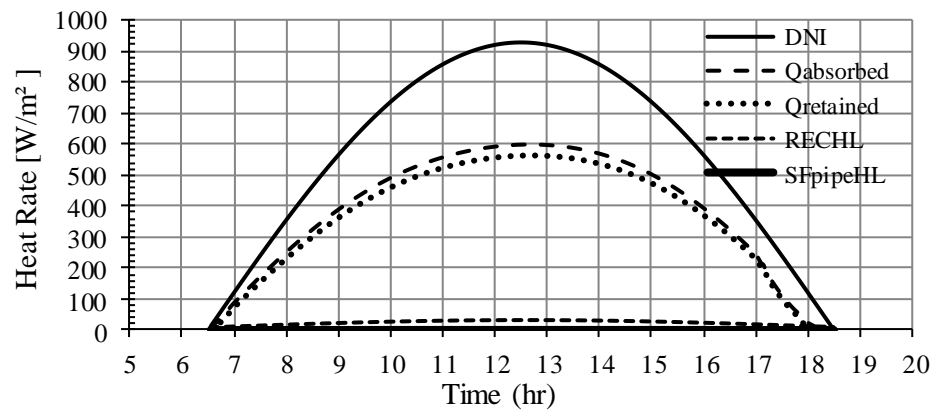


Figure 4.11: Rates of heat absorption and heat loss from the solar field for august 16.

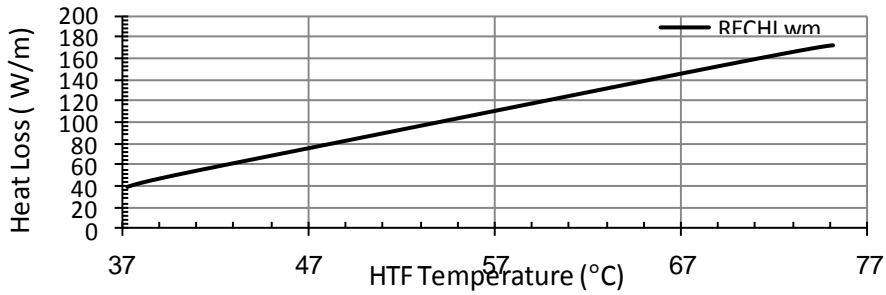


Figure 4.12. Receiver heat loss vs. bulk fluid temperature

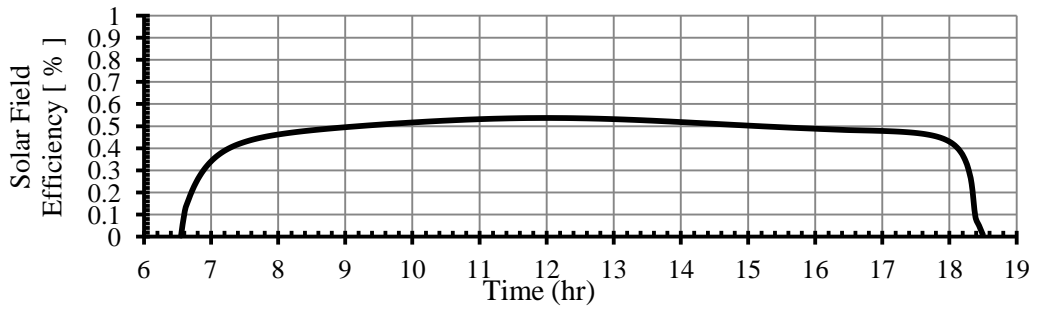


Figure 4.13 Solar Field Efficiency Variation during operation hours of august 16.

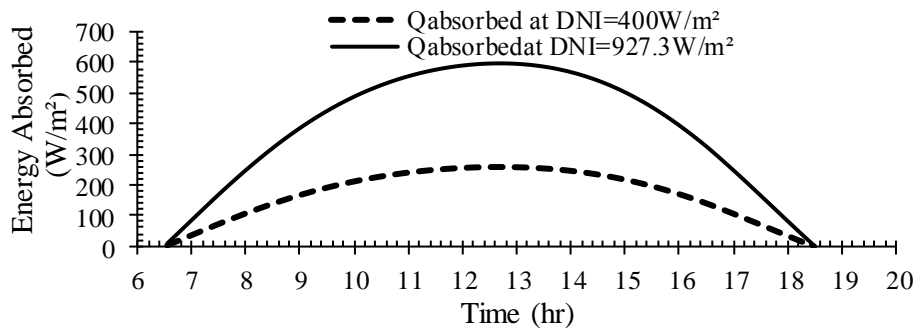


Figure 4.14: Effect of Direct Normal Insolation on Energy absorbed by Solar Field.

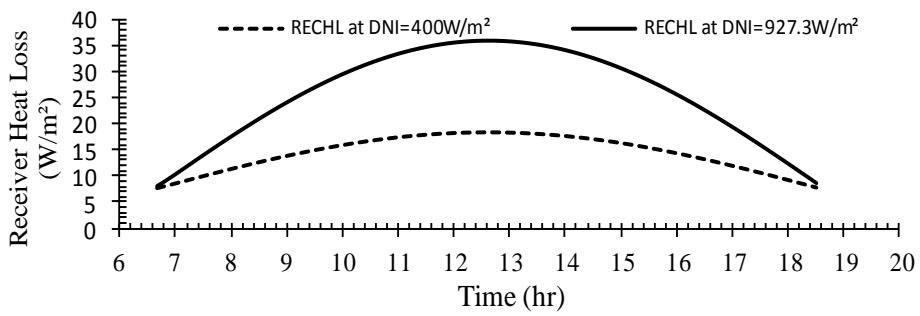


Figure 4.15: Effect of Direct Normal Insolation on Receiver Heat Loss.

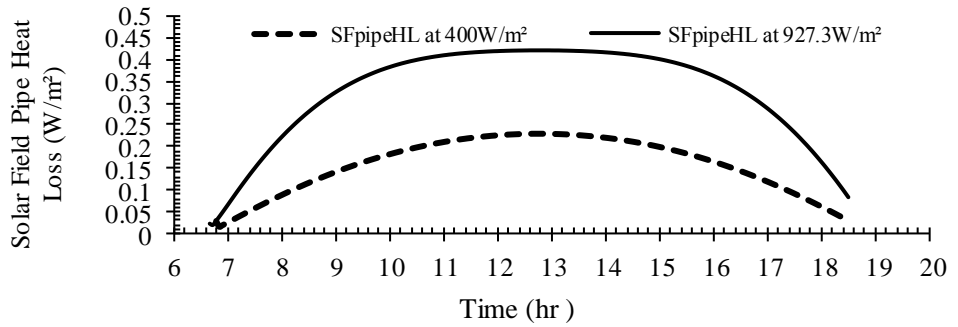


Figure 4.16: Effect of Direct Normal Insolation on Solar Field Pipe Heat Loss.

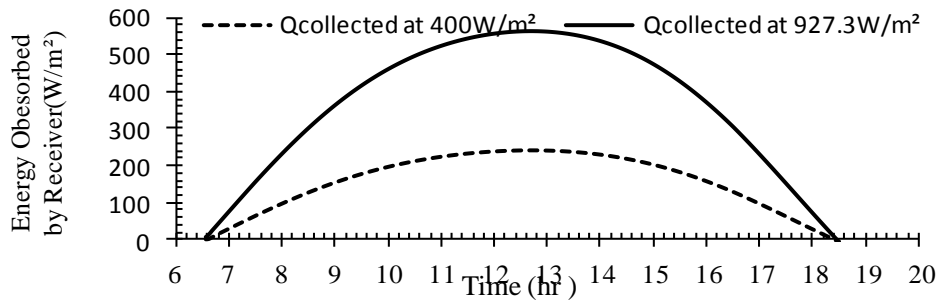


Figure4.17:Effect of Direct Normal Insolation on Energy absorbed by Receiver.

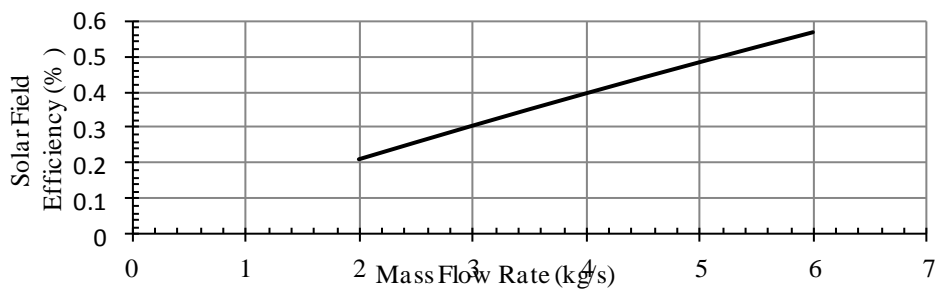


Figure 4.18: Effect of Mass Flow Rate on the Solar Field Efficiency

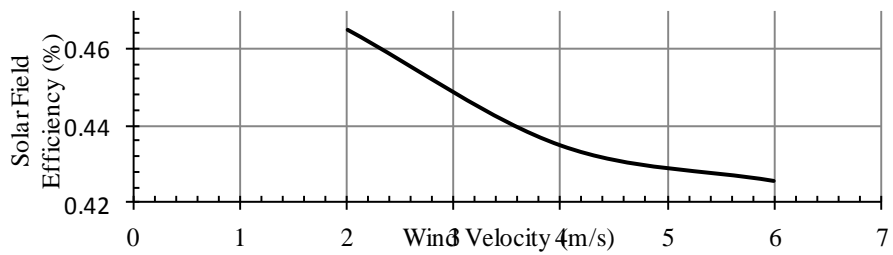


Figure 4.19: Effect of Wind Velocity on Solar Field Efficiency.

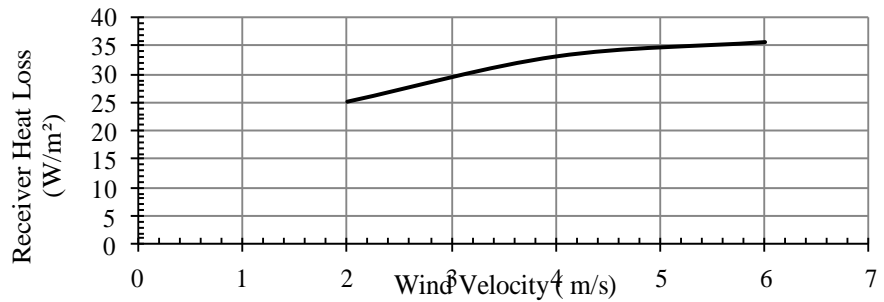


Figure 4.20: Effect of Wind Velocity on Receiver Heat losses.

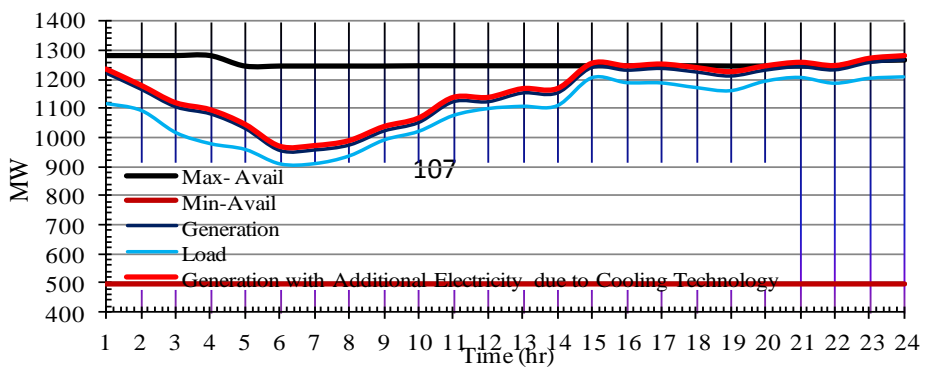


Figure 4.21: Libyan Eastern Network Daily Load Curve August 16.

Table4.1: Capacity increase for the considered combined cycle unit for a cooling capacity of 9.1193 MW and a design compressor inlet temperature of 15 °C

Month	Average Max Air Temp. (°C)	Actual OH of GTI (HR)	GTI Actual Power(MW) Cooler OFF	GTI Power (MW) Cooler ON	Additional electric Energy (MWh)	ST ₂₂ Actual Power (MW)	Average Max Sea Temp. (°C)	Actual OH of ST ₂₂ (HR)	Additional electric Energy (MWh)
Jan	17	728	122.7	128.3	-	113.9	19	560	464.8
Feb	18	672	127.9	128.3	-	115.3	18	670	-
Mar.	20	744	119.9	128.3	6349.6	126.2	18	670	-
Apr.	25	744	117.6	128.3	7639.8	123.5	20	712	1181.92
May	29	727	120.5	128.3	5670.6	133.1	21	744	1852.56
June	32	720	114.6	128.3	9864	135.6	24	712	3545.76
July	32	744	116	128.3	9151.2	136.1	27	744	5557.68
Aug.	32	736	115.8	128.3	9200	135.9	27	744	5557.68
Sep.	31	720	116	128.3	8856	137.2	27	720	5378.4
Oct.	28	744	103	128.3	18823.2	85.2	26	611	4057.04
Nov.	24	685	81.6	128.3	31989.5	83.8	25	695	4037.95
Dec.	19	744	109.5	128.3	-	117.3	22	687	2280.84

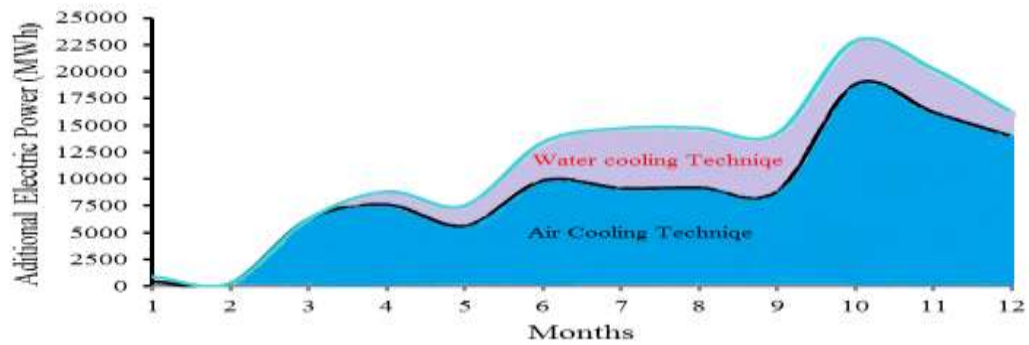


Figure 4. 22: Total effect of Cooling Technology on Combined Cycle Monthly Electrical Energy Production Enhancement.

Table 4.2 The annual fraction of load covered by the solar energy system

	Month	X	XC	Y	f	L(GJ)	f*L(GJ)
1	January	50.03	1	22.47	1	323.144	323.144
2	February	157.43	1	98.74	1	91.638	91.638
3	mars	12.71	1	9.67	1	1226.038	1226.038
4	April	4.48	1	4.04	1	3153.171	3153.171
5	May	2.77	1	2.52	1	4989.543	4989.543
6	June	1.22	1	1.56	0.874	10516.306	9191.251
7	July	1.17	1	1.24	0.867	11359.132	9848.367
8	August	1.09	1	1.14	0.818	12139.587	9930.182
9	September	1.57	1	1.59	1	8263.728	8263.728
10	October	2	1	1.66	1	6999.434	6999.434
11	November	4.82	1	43.26	1	2973.622	2973.622
12	December	71.22	1	33.49	1	221.531	221.531

The annual fraction of load covered by the solar energy system

from the table 4.2 is[42]: $F = \frac{\sum f_i L_i}{\sum L_i}$

$$F = 57211.649 / 62256.874 = 0.91896$$

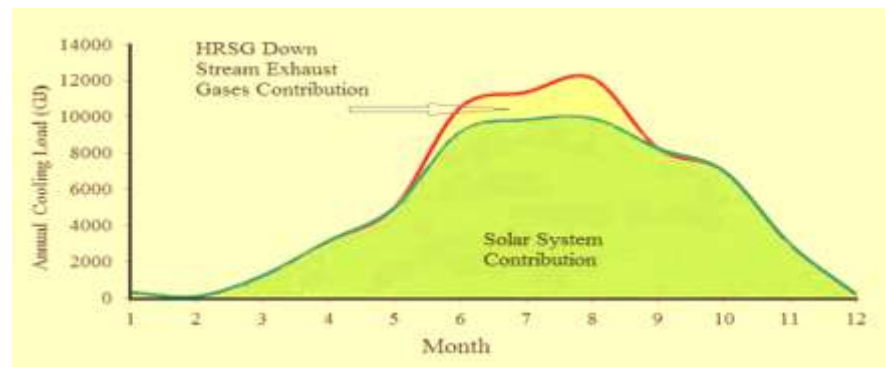


Figure 4. 23: Contribution of Solar System Integrated with HRSG Waste Heat Covering Annual Cooling Load of Benghazi North Power Plant Intake Air

4.1. Estimation of initial, operation and maintenance costs:

The initial costs of the modeled components, in the current study, were either calculated or obtained from official sources or past studies. The fixed cost elements were then entered directly into the total capital investment subsection of the investment [35] .

Table 4.3: Total Cost of Cooling Unit.

Component	Price (\$)	Reference
Absorption Chiller (2606 RT)	1,443,298	34
Compact Heat Exchanger	385,195	34
Chilled Water Pump	977,890.36	35
Condensate Pump	83,281	35
Control System	486,258	35
Miscellaneous	444,648	35
Storage Tank chilled water and Chilled Water Pump	6,138,684.36	34
Solar Field	7,749,355	36
Auxiliary heater	405,000	34
Storage Tank hot water with pump	341,377	34
12% of total cost(installations)	2,214,598.4	34
Operation and Maintenance Annual Cost		
Operation	11,430	36
Maintenance	171,980.68	37,35
Power Supply To The Cooling Water System	21,980	36

Table 4.4 The annual energy revenues

Model	8489 hrs (Whole year)at variable selling price (0.05 – 0.33 \$/kWh)		
	Additional Electrical energy (kWh)	Selling price (\$/kWh)	Revenue(\$)
single effect	141,358,530	0.05	7,067,926.5
		0.08	11,308,682.4
		0.1	14,135,853
		0.2	28,271,706
		0.33	46,648,314.9

Annual savings = Revenues -Total operating and maintenance cost.

PB = Total capital cost / Annual savings.

Figure 4.23 illustrates the effects of the variations of the selling prices on the payback period profitability measures. When the selling price increased from \$ 0.05 to 0.33 per kWh, the pay back were 3.0119, 1.8616, 1.4838 , 0.7365and 0.4451 years respectively.

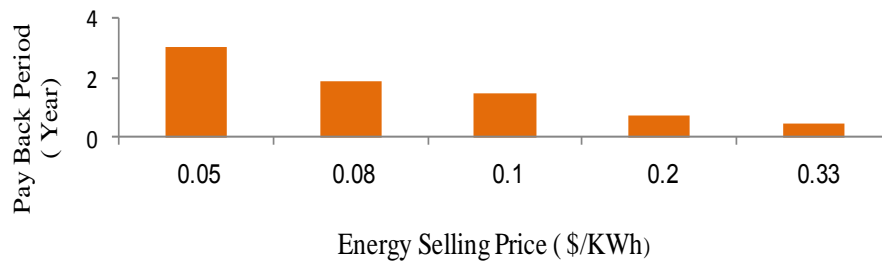


Figure 4.23: Payback Period Versus Variation of The Energy Selling Prices

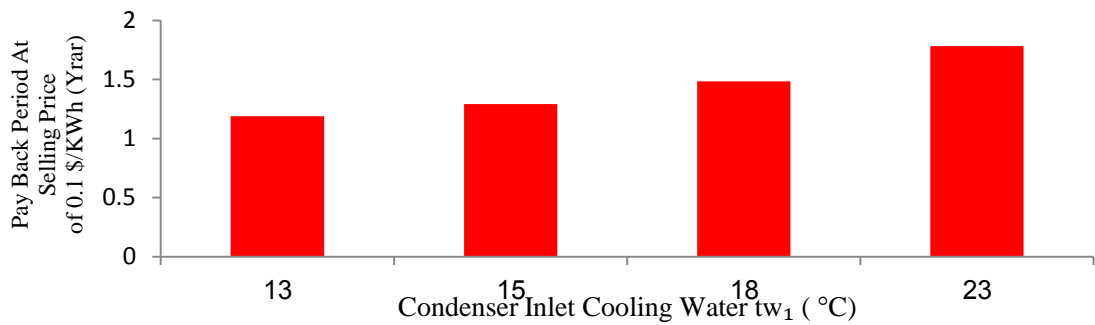


Figure 4.24: Effect of Condenser Inlet Cooling Water on Payback Period.

Figure 4.24 illustrates the effects of the condenser inlet cooling water temperature (t_{w1}) variations on the payback period profitability measures at constant selling price of 0.1 \$/kWh . When the condenser inlet cooling water temperature (t_{w1}) decreased from 23 °C to 13 °C, the pay back were 1.7821, 1.4838, 1.2927 , and 1.1905 years respectively.

4.2. Final Saving

The estimated net electricity production in the present work would increase by 107,443.9 MWh/yr due to intake air cooling technology alone, while 61,826.3 MWh/yr was achieved by Aziza [35]. The

estimated net electricity production due to condenser inlet cooling water cooling technology would increase by 10,596.61 MWh/yr when t_{w1} cooled from 27 °C to 23 °C, 33,914.63 MWh/yr when t_{w1} cooled from 27 °C to 18 °C, 54,504.44 MWh/yr at $t_{w1} = 15$ °C, and 68,230.98 MWh/yr at $t_{w1} = 13$ °C which can finally save money by around 11,804,051 \$/yr, 14,135,853 \$/yr, 16,194,834 \$/yr and 17,567,488 \$/yr respectively with electricity selling price of 0.1 \$/kwh.

4.3. CO₂ Treatment Saving:

One of CO₂ treatment methods is planting trees and this costs money. By CIAC, and CICWCT this cost can be saved in terms of trees planting as can be seen from figure 4.25

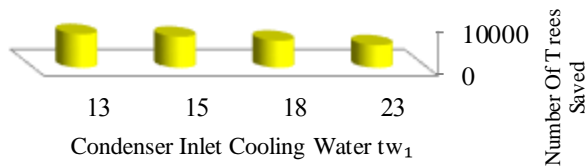


Figure 4.25: Effect of Condenser Inlet Cooling Water on The Number Of Trees Saved.

Figure 5.4 shows the effect of condenser inlet cooling water on the number of trees saved in the scenario of the CO₂ treatment when t_{w1} decreased from 27 °C to 13 °C the emission of CO₂ decreased from 373.412 g_{CO2}/kWh to 363.886 g_{CO2}/kWh and there for the cost of CO₂ treatment which presented in planting of trees also decreased.

For every one fully grown tree on average consumes 12 kg of CO₂ annually. The additional electric energy achieved causes CO₂ treatment savings and this treatment represented in planting trees.

Number of trees saved = Amount of CO₂ saved (tones) / 12

When the condenser cooling water temperature lowered from 27 °C to 18 °C the saved trees can be calculated as follows :

Number of trees saved = $(141,358.53 \times 10^3 \text{ kWh}) \times (0.53 \text{ KgCO}_2/\text{kWh}) \times 10^{-3} / 12 = 6243.34$ Trees. The social cost due to CO₂ emissions is 220 \$, so the saved money

The money saved = $[(141,358.53 \times 10^3 \text{ kWh}) \times (0.53 \text{ KgCO}_2/\text{kWh}) \times 10^{-3}] \times 220$.

The money saved = 16,482,405 \$.

5. Conclusion and Recommendations

All the results obtained from this study indicate that modifying an existing combined gas steam turbine power plant, currently operating in Benghazi Libya, to include inlet air cooling and the condenser inlet cooling water will have beneficial effects. The literature review indicated that Absorption refrigeration cooling was the most attractive option as it could make use of energy in the plant exhaust stand alone or supported with clean source of energy such as solar energy. The model predicted

the proposed plant would work in a stable and efficient condition at base load. This study has shown that using an absorption chillier for cooling the gas turbine air inlet and the condenser inlet cooling water will increase the peak capacity of the plant during the hot ambient operation by increasing the density of the mass flow rate and increasing the vacuum in the steam turbine condenser and improving the output power.

The main results obtained can be concluded as follows:

1. It can be seen that the power output of the gas turbine stand alone and combined cycle plant declined by 0.688 % and 0.556 % for each 1°C ambient temperature rise when the ambient air temperature rises from 5 °C to 50 °C. By inlet air cooling from 37 °C to ISO condition the power output improved by 0.662 % and 0.475 % respectively.
2. At base load when the ambient air temperature rises from 5 °C to 50 °C, the gas turbine stand alone and combined cycle thermal efficiencies dropped by 0.242 % and 0.072 % respectively for each 1°C ambient temperature rise. When the inlet air was cooled from 37 °C to ISO condition the gas turbine stand alone and combined cycle plant efficiencies improved by 5.84 % and 2.03 % also The inlet air cooling system helps to reduce environmental pollution as the specific fuel consumption is less than that of gas turbine standalone and CCPP by 5.52%, and 2% respectively. Calculation and modeling shows that the variation of the air inlet temperature from 37°C to 15°C generates a

reduction of 7.13% % in the compressor work, and this leads to reduce fuel consumption in combustion chamber by 8.2%.

3. The seawater temperature was also found to have a significant effect on the generated power. when the condenser inlet cooling water dropped from 27 °C to 8 °C The power output and thermal efficiency increased by of 3.666 % and 3.595 % respectively and the CO₂emission released to the environment reduced by 3.558%.

4. The use of the solar system aided with thermal storage tank to a drive the absorption unit for cooling the intake air can be considered as a reliable energy source where the annual solar fraction or the solar contribution reached 91.89 %.

5. The HTF mass flow rate , solar insolation, and wind velocity has an effect on solar field power gain, efficiency, receiver heat loss solar field piping losses.

6. Angle of incidence θ has a strong effect on the absorbed energy by parabolic collector while HTF bulk temperature has a linear effect on Receiver heat loss also the ratio between zenith angle (θ_z) and angle of incidence θ effect on row shadow factor which effect on the absorbed energy and the angle of incidence θ has an effect on the end loss.

7. The present study has concluded that the cooling of the intake air entering the gas turbine compressor will increase the power output by 9.767 % for the gas turbine standalone and 7.728% for the combined

cycle plant annually and the net electricity production increases by 141,358,530MWh/yr, which has a positive effect on the electricity national grid, the eastern electricity grid, and the daily load curve and minimize the periods of disconnections.

8. By cooling the intake air and condenser inlet cooling water leads to stabiles the circumferences of the operation which positively affect the performance and the efficiency throughout the life span and leads to increase the life of the plant.

References:

- [1] Amir A. Zadpoor, Ali H. Golshan, "Performance improvement of a gas turbine cycle by using a desiccant-based evaporative cooling system", Available at: Science Direct www.elsevier.com/locate/energy. (Accessed 14 December 2018).
- [2] Suleiman, Rekiyat B. Omohu, " Modeling And Simulation Of A Solar Powered Adsorption Refrigeration System", June 2011.
- [3] Ashraf Khalil, Zakaria Rajab, Ali Asheibi. The Economic Feasibility of Photovoltaic Systems for Electricity Production in Libya.Hammamet, Tunisia : s.n., 2016. The 7th International Renewable Energy Congress (IREC'2016). pp. 1-6.

- [4] Ibrahim M. Saleh " Prospects of Renewable Energy in Libya" , International Symposium on Solar Physics and Solar Eclipses (SPSE) 2006.
- [5] Abdulwahab Misherghi," Renewable Energy in Libya: (Potentials, Current Situation and Way forward), Berlin - Germany, Monday 26th of June 2012.
- [6] Lawrence Livermore National Laboratory, "*Energy Flow Charts*". 2016 [cited 2017 Dec 15]; Available from: <https://flowcharts.llnl.gov/>
- [7] Institute, G.C. Power Plant Efficiency. 2018 [cited 2018 Feb 11]; Available from: <https://hub.globalccsinstitute.com/publications/capturing-co2/power-plant-efficiency>.
- [8] dos Santos AP, Andrade CR, Zaparoli EL. "Comparison of different gas turbine inlet air cooling methods". World Academy of Science, Engineering and Technology. 2012 Jan 26;61:40-5.
- [9] Ibrahim TK, Rahman MM, Abdalla AN." Improvement of gas turbine performance based on inlet air cooling systems: A technical review". International Journal of Physical Sciences. 2011 Feb 18;6(4):620-7.
- [10] Raja FA, Christofer SB, Rajan A, Thiagarajan TC." Frequency Excursion and Temperature control of Combined

- Cycle Gas Plant Including SMES". International Journal of Computer and Electrical Engineering. 2010 Dec 1;2(6):1059.
- [11] Tiwari AK, Hasan MM, Islam M." Effect of Operating Parameters on the Performance of Combined Cycle Power Plant". 1 (7) 2012.
- [12] Muammer Alus, Mohamed Elrawemi, Fathi Kawan, "The Effect of the Condenser Inlet Cooling Water Temperature on the Combined Cycle Power Plant Performance", World Wide Journal of Multidisciplinary Research and Development, WWJMRD 2017; 3(10): 206-21.
- [13] Waiel Kamal,etal " Effect of Inlet Air Cooling on Gas Turbine Performance" Bandar Seri Iskandar, 31750 Tronoh, Perak, Malaysia University of Technology Petronas no date.
- [14] Kamal, S. N. O., Salim, D. A., Fouzi, M. S. M., Khai, D.T. H., and Yusof, M. K. Y., "Feasibility study of turbine inlet air cooling using mechanical chillers in malaysia climate", International Conference on Alternative Energy in Developing Countries and Emerging Economies AEDCEE, Bangkok, Thailand, 25-26 May, 2017.
- [15] A.E.M. Nasser, M.A. EI-Kalay, "A heat-recovery cooling system to conserve energy in gas-turbine power stations in the Arabian Gulf", Appl. Energy 38 (1991) 133–142.

- [16] Johansson, T.B. "Renewable Energy, Sources for Fuels and Electricity"; Island Press: Washington, DC, USA, 1993;Chapter 5, pp. 234–235.
- [17] Zhu, G., Neises, T., Turchi, C., Bedilion, R. "Thermodynamic evaluation of solar integration into a natural gas combined cycle power plant". *Renew. Energy* 2015, 74, 815–824.
- [18] Lewis, N. "Toward cost-effective solar energy use". *Science* 2007, 315, 798–801.
- [19] Behar, O.; Kellaf, A.; Mohamedi, K.; Belhamel, M. "Instantaneous performance of the first Integrated Solar Combined Cycle System in Algeria". *Energy Procedia* 2011, 6, 185–193.
- [20]Rovira, A.; Montes, M.J.; Varela, F.; Gil, M. "Comparison of Heat Transfer Fluid and Direct Steam Generation technologies for Integrated Solar Combined Cycles". *Appl. Therm. Eng.* 2013, 52, 264–274.
- [21] Montes, M.J.; Rovira, A.; Muñoz, M.; Martínez-Val, J.M. "Performance analysis of an Integrated Solar Combined Cycle using Direct Steam Generation in parabolic trough collectors". *Appl. Energy* 2011, 88, 3228–3238.
- [22] Baghernejad, A.; Yaghoubi, M. "Exergoeconomic analysis and optimization of Integrated Solar Combined Cycle System

- (ISCCS) using genetic algorithm". *Energy Convers. Manag.* 2011, 52, 2193–2203.
- [23] Baghernejad, A.; Yaghoubi, M. "Exergy analysis of an integrated solar combined cycle system". *Renew. Energy* 2010, 35, 2157–2164.
- [24] Bakos, G.C.; Parsa, D. "Technoeconomic assessment of an integrated solar combined cycle power plant in Greece using line-focus parabolic trough collectors". *Renew. Energy* 2013, 60, 598–603.
- [25] Li, Y.; Yang, Y. "Thermodynamic analysis of a novel integrated solar combined cycle". *Appl. Energy* 2014, 122, 133–142.
- [26] Li, Y.; Yang, Y. "Impacts of solar multiples on the performance of integrated solar combined cycle systems with two direct steam generation fields". *Appl. Energy* 2015, 160, 673–680.
- [27] Popov, D. "An option for solar thermal repowering of fossil fuel fired power plants". *Sol. Energy* 2011, 85, 344–349.
- [28] Popov, D. "Innovative solar augmentation of gas turbine combined cycle plants". *Appl. Therm. Eng.* 2014, 64, 40–50.
- [29] Liqiang Duan and Zhen Wang "Performance Study of a Novel Integrated Solar Combined Cycle System" *Energies* 2018, 11, 3400; doi:10.3390/en11123400 .

- [30] Ahmed Ali Abdel Rahman "Boosting Gas Turbine Combined Cycles in Hot Regions Using Inlet Air Cooling including Solar Energy",9th International Conference on Applied Energy, ICAE2017, 21-24 August 2017, Cardiff, UK.
- [31] S. Popli, P. Rodgers, V. Eveloy, "Gas turbine efficiency enhancement using waste heat powered absorption chillers in the oil and gas industry", Appl. Therm. Eng. 50 (2013) 918–931.
- [32] Erkinjon Matjanov "Gas turbine efficiency enhancement using absorption chiller. Casestudy for Tashkent CHP" Energy. 192 (2020) 116625. Elsevier Ltd.
- [33] V.C. Okafor " Thermodynamic Analysis Of Compressor Inlet Air Precooling Techniques Of A Gas Turbine Plant Operational In Nigeria Energy Utility Sector" International Journal of Engineering Science Technologies Vol. 4(2): March, 2020.
- [34] A. Ettajuri et.al " Unsteady Thermal performance of Solar Parabolic Trough Collector Integrated With HRSG Exhaust Gases Under Different Loading Conditions of Benghazi North Power Plant " Master of Science University of Benghazi Thesis April 2021.
- [35] Aziza Salem Abdelatif" Theoretical Investigation of the Gas Turbine Performance Enhancement by Intake Air Cooling

Using An Absorption Chiller", The Libyan Academy Benghazi
- Libya .2018.

- [36] Erkinjon Matjanov "Gas turbine efficiency enhancement using absorption chiller. Casestudy for Tashkent CHP" Energy. 192 (2020) 116625. Elsevier Ltd.
- [37] Ameri, M. and S.H. Hejazi, "The study of capacity enhancement of the Chabahar gas turbine installation using an absorption chiller". Applied Thermal Engineering, 2004. **24**(1): p. 59-68.
- [38] Giama M. Fellah., Effect of Ambient Temperature on The Thermodynamic Performance of A combined Cycle", Journal of Engineering Research (Al-Fateh University) Issue (13) March 2010.
- [39] Nasser, A.E.M. and M.A. Elkalay, "A heat-Recovery Cooling System to Conserve Energy in Gas-Turbine Power-Stations in The Arabian Gulf". Applied Energy, 1991. **38**(2): p. 133-142.).
- [40] Santos AP, Andrade CR. "Analysis of gas turbine performance with inlet air cooling techniques applied to Brazilian sites". Journal of Aerospace Technology and Management. 2012 Sep;4(3):341-353.

- [41] Q.M. Jaber et al, "Assessment of power augmentation from gas turbine power plants using different inlet air cooling systems" ,Jordan J. Mech. Ind. Eng. 1 (1) (2007) 7–15.
- [42] Abdel Moneim, S.A., " No-Load Unsteady- State Thermal Performance of Parabolic Trough Solar Collectors 5 , "th International Conference on Energy and Environment, Cairo, Egypt, 1996.
- [43] Soteris kalogirou "Solar energy engineering" 1st. ED., Elsevier Inc. 2009.

Appendix A

Air Compressor Model:

$$rp = \frac{p_2}{p_1}, \quad \eta_c = \frac{T_{2s} - T_1}{T_2 - T_1}, \quad T_{2s} = T_1 * (rp)^{\frac{\gamma_a - 1}{\gamma_a}}, \quad T_2 = T_1 * \left(1 + \frac{rp^{\frac{\gamma_a - 1}{\gamma_a}} - 1}{\eta_c}\right)$$

$$W_c = \frac{C_{pa} * T_1 * (rp^{\frac{\gamma_a - 1}{\gamma_a}} - 1)}{\eta_c * \eta_m}$$

Combustion Chamber model:

$$\dot{m}_a * C_{pa} * T_2 + \dot{m}_f * LHV + \dot{m}_f * C_{pf} * T_f = TIT * C_{pg} * (\dot{m}_a + \dot{m}_f),$$

$$f = \frac{\dot{m}_f}{\dot{m}_a} = \frac{C_{pg} * TIT - C_{pa} * T_2}{LHV - C_{pg} * TIT}$$

Gas Turbine Mode

$$W_t = C_{pg} * TIT * \eta_t * R_{pg} / \eta_m, \quad W_{net} = W_t - W_c,$$

$$T_4 = T_3 * (1 - \eta_t * R_{pg})$$

$$Q_{add} = C_{pg} * (TIT - T_1 * (1 + R_{pg})), \quad \eta_{th} = \frac{W_{gnet}}{Q_{add}}, \quad HR = \frac{3600}{\eta_{th}}$$

Steam Turbine Model

$$Q_{av} = \dot{m} * C_{pg} * (T_{g1} - T_{g4}) * h_{1f} \quad , \quad W_{st} = \dot{m}_s * (h_6 - h_7) \quad , \quad Q_{cond} = \dot{m}_w * (h_7 - h_8) \quad , \quad W_p = \dot{m}_w * v_{fg} * (p_{sh} - p_c)$$

$$W_{snet} = W_{st} - W_p \quad , \quad \eta_{st} = W_{snet} / Q_{av} \quad , \quad \eta_{all} = (W_{net} + W_{snet}) / Q_{add} \quad , \quad HR_t = 3600 / \eta_{all}$$

Condenser Inlet Cooling Water Temperature Controlling

$$t_s = t_{w1} + TR + TTD \quad , \quad Q_{sT} = \dot{m}_{st} * (h_6 - h_1) \quad ,$$

$$Q_w = \dot{m}_w * C_{pw} * (t_{w2} - t_{w1})$$

Absorption Cycle

$$X_1 = X_2 = X_3 = X_w \quad , \quad X_4 = X_5 = X_6 = X_s$$

At the absorber:

$$\dot{m}_1 = \dot{m}_{10} + \dot{m}_6 \quad , \quad \dot{m}_1 X_1 = \dot{m}_6 X_6$$

$$\dot{Q}_a = \dot{m}_6 h_6 + \dot{m}_{10} h_{10} - \dot{m}_1 h_1$$

Combined cycle [27]

At the generator:

$$\dot{m}_3 = \dot{m}_7 + \dot{m}_4 \quad , \quad \dot{m}_3 X_3 = \dot{m}_4 X_4$$

$$\dot{Q}_g = \dot{m}_4 h_4 + \dot{m}_7 h_7 - \dot{m}_3 h_3$$

At the condenser:

$$\dot{m}_7 = \dot{m}_8 = \dot{m}_{ref} \quad , \quad \dot{Q}_c = \dot{m}_{ref} * (h_7 - h_8)$$

At the evaporator:

absorption

$$\dot{m}_9 = \dot{m}_{10} = \dot{m}_{ref} \quad , \quad \dot{Q}_e = \dot{m}_{ref} * (h_{10} - h_9)$$

At the solution heat exchanger:

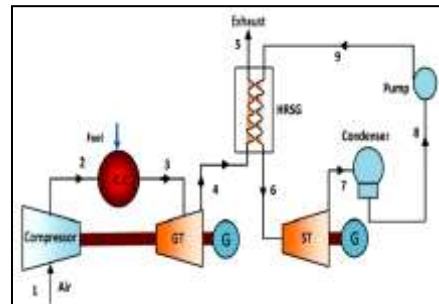


Figure 3.3:

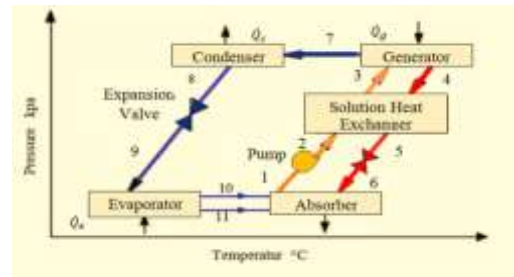


Figure 3.5: Schematic diagram of basic refrigeration cycle [50]

$$\dot{m}_2 + \dot{m}_4 = \dot{m}_3 + \dot{m}_5$$

$$\dot{m}_2 h_2 + \dot{m}_4 h_4 = \dot{m}_3 h_3 + \dot{m}_5 h_5, \quad \varepsilon = \frac{h_4 - h_5}{h_4 - h_2},$$

$$h_{sol} = \sum_{i=0}^4 c_i x^i + T_{sol} \sum_{i=0}^4 d_i x^i + T_{sol}^2 \sum_{i=0}^4 e_i x^i \quad COP = \frac{\dot{Q}_e}{\dot{Q}_g} \quad \dot{Q} = \varepsilon * C_{min} (T_{hot,in} - T_{cold,in})$$

$$\varepsilon = \frac{\dot{Q}}{\dot{Q}_{max}} \quad NTU = f\left(\varepsilon, \frac{C_{min}}{C_{max}}\right)$$

Cooling load estimation for gas turbine inlet cooling

$$Q_s = (V_{dota}/V_a) * C_{pa} * (t_{aadb} - t_{ci}), \quad V_a = (0.287 + X_{aadb} * 0.462) * (T / P_{atm})$$

$$X_{aadb} = (P_s / ((P_{atm}/R_h) - P_s)) * (M_v/M_a),$$

$$Q_l = (V_{dota}/V_a) * (X_{aadb} * (C_{pv} * t_{aadb} + r) - X_{sci} * (C_{p,v} * t_{ci} + r)) - (X_{aadb} - X_{sci}) * C_{p,w} * t_{ci}$$

$$X_{sci} = (P_{s1}/(P_{atm} - P_{s1})) * (M_v/M_a), \quad Q_c = Q_s + Q_l, \quad A = Q_c / (U * \Delta T_{in} * F)$$

$$\Delta T_{in} = ((T_{amb} - T_{chwr}) - (T_{iso} - T_{chws})) / \ln [(T_{amb} - T_{chwr}) / (T_{iso} - T_{chws})]$$

$$\text{Thermal energy storage system (TES)} \quad V_{gross} = V_{theory} / 0.8$$

$$V_{theory} = \text{TES capacity in ton-hours} * 3.024 / (T_{chwr} - T_{chws})$$

$$\dot{m}_{chw} = \dot{m}_{air} * C_{pair} * (T_1 - T_2) / (C_{pw} * (T_{chwr} - T_{chws}))$$

Solar radiation estimation

$$\text{The length of day estimation:} \quad td = 2/15 * \cos^{-1} [-\tan \phi_L * \tan \delta]$$

$$\text{Sunrise and sunset calculations:} \quad \omega_s = \cos^{-1} [-\tan \delta \tan \phi_L]$$

$$H_{sr} = 12 - \frac{\omega_s}{15} \quad H_{sr} = 12 + \frac{\omega_s}{15}$$

The sun tracking system

$$\cos(\theta) = \sqrt{\cos^2 \theta_z + \cos^2 \delta \cdot \sin^2 \omega}$$

Incidence Angle Modifier (IAM)

$$IAM = 1 + 0.000884 \frac{\theta}{\cos(\theta)} - 0.00005369 \frac{\theta^2}{\cos(\theta)}$$

Row Shadowing and End Losses

$$\text{Row Shadow} = \frac{L_{\text{spacing}}}{W} + \frac{\cos(\theta_z)}{\cos(\theta)}$$

The end losses

$$\text{End Loss} = 1 - \frac{f \tan(\theta)}{L_{\text{SCA}}}$$

Field Efficiency and HCE Efficiency

$$\eta_{\text{LF}} = \sum_{i=1}^{N_{\text{traces}}} \text{ColFrac}_i \cdot \text{TrkTwstErr}_i \cdot \text{GeoAcc}_i \cdot \text{MirRef}_i \cdot \text{MirCln}_i$$

Receiver Heat Loss

$$HL_{\text{field}} = \frac{a_0 (T_0 - T_1) + \frac{a_1}{2} (T_0^2 - T_1^2) + \frac{a_2}{3} (T_0^3 - T_1^3) + \frac{a_3}{4} (T_0^4 - T_1^4) + \text{DNI} \left[b_0 (T_0 - T_1) + \frac{b_1}{3} (T_0^3 - T_1^3) \right]}{T_0 - T_1}$$

$$\text{ReCHL} = \sum_{i=1}^{N_{\text{traces}}} \text{HCEFrac}_i \cdot \frac{HL_{\text{field},i}}{\text{Width}}$$

Solar Field Piping Heat Losses

$$\text{SPipe}_{\text{eff}} = 0.01693 \Delta T + 0.0001683 \Delta T^2 + 6.78 \cdot 10^{-7} \Delta T^3 \quad \Delta T = \frac{T_{\text{recolcol}} + T_{\text{recolrow}}}{2} - T_{\text{ambent}}$$

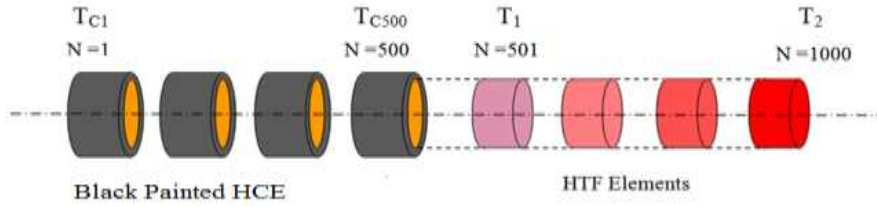


Figure 3.27: Receiver Tube Divided Into Elements

Black coated tube receiver
$$\frac{\partial T_c}{\partial t} = \frac{1}{\rho_c C_p V_c} (\alpha_c \eta_{opt} A_a DNI - U A_{s,o} (T_c - T_\infty) - h_r A_{s,i} (T_c - T_f))$$

where , $T_c = T_{c(x,t)}$, $T_f = T_f$, $A = B \cdot L$, $A_{s,i} = \pi d_i \Delta x$, $A_{s,o} = \pi d_o \Delta x$, $V_c = \pi/4 (d_o^2 - d_i^2) \Delta x$ and $U = h_w + h_{rad}$, $h_i = 81 + 9m^{0.8} T_f$, $h_w = 5.7 + 3.8V_w$ and $h_{rad} = \epsilon \sigma (T_s^2 + T_\infty^2)(T_s + T_\infty)$ [152] .

direct normal Insolation DNI
$$DNI = I'' \sin \left(\frac{\pi t}{12} \right)$$

flowing Fluid element
$$\frac{\partial T_f}{\partial t} = \frac{1}{\rho_f C_p V_f} (m C_p (T_1 - T_2) + h_r A_{s,i} (T_c - \frac{1}{2}(T_1 + T_2)))$$

Storage Tank
$$\frac{dT_{st}(t)}{dt} = \frac{1}{\rho_f C_p V_{st}} m C_p (T_{st}(t) - T_{st}(t))$$

Initial Conditions

a. For receiver tube walls; $T_c(x,0) = T_\infty$, for $x = 0$ to L

b. For fluid ; $T_1(x,0) = T_2(x,0) = T_f(x,0) = T_\infty$, for $x = 0$ to L

c. For the stored fluid ; For lumped model $T_{st.}(0) = T_{\infty}$

Boundary Conditions

1.For receiver tube walls; $T_c(0,t) = T_{st.}(t)$, for t = 0 to 12 hr.

2. For fluid ; $T_1(0,t) = T_{st.}(t)$, for t=0 to 12 hr.

Solar Irradiation Absorption

$$Q_{\text{absorbed}} = \text{DNI} \cdot \text{COS}\theta \cdot \text{IAM} \cdot \text{ROW}_{\text{Shadow}} \cdot \text{End}_{\text{Loss}} \cdot \eta_{\text{S.F}} \cdot \eta_{\text{HCE}} \cdot \text{SF}_{\text{Avail}}$$

$$\text{HTF Energy Gain and Temperature Rise } Q_{\text{collected}} = Q_{\text{absorbed}} - (\text{Re}_{\text{cHL}} + \text{SfPipe}_{\text{HL}})$$

Solar Field, Power Cycle Efficiency

$$Q_{\text{COL}} = \dot{m}_{\text{HTF}} (h_{\text{SF,out}} - h_{\text{SF,in}}) , \text{Incident} = \text{DNI} \cdot \text{COS} \theta \cdot \text{IAM}$$

$$\text{DC} = \frac{86.4 \cdot 10^3 \cdot Q_{\text{C}}}{T_o - T_i} \quad (\text{DD})_{\text{C}}$$

Annual load supplied by the solar energy system

$$\text{Emission of greenhouse gases. } (\text{Emission})_{\text{CO}_2} = E_{\text{W}} * \text{FG} * \Delta t * N$$

$$\text{Determination of the solar collector surface area } . A_{\text{c}} = \frac{Q_{\text{g}}}{I_{\text{p}} * \eta_{\text{c}}}$$

Estimating of the monthly average daily total radiation and day period for Benghazi city.

$$h_{\text{ss}} = \cos^{-1}[\tan(L) \tan(\delta)] , h'_{\text{s}} = \min\{h_{\text{ss}}, \cos^{-1}[-\tan(L - \beta) \tan(\delta)]\}$$

$$\bar{R}_{\text{B}} = \frac{\cos(L - \beta) \cos(\delta) \sin(h'_{\text{ss}}) + (\pi/180) h'_{\text{ss}} \sin(L - \beta) \sin(\delta)}{\cos(L) \cos(\delta) \sin(h_{\text{ss}}) + (\pi/180) h_{\text{ss}} \sin(L) \sin(\delta)}$$

$$\bar{R} = \frac{\bar{H}_{\text{D}}}{\bar{H}} = \left[1 - \frac{\bar{H}_{\text{D}}}{\bar{H}} \right] \bar{R}_{\text{B}} + \frac{\bar{H}_{\text{D}}}{\bar{H}} \left[\frac{1 + \cos(\beta)}{2} \right] + \rho_{\text{g}} \left[\frac{1 - \cos(\beta)}{2} \right]$$

Estimation of solar contribution (solar factor)

$$X = F_R U_L * \frac{F_R'}{F_R} (T_{ref} - \overline{T_a}) * \Delta t * \frac{A_c}{l}, \quad Y = F_R (\tau\alpha)_n * \frac{F_R'}{F_R} * \left[\frac{(\tau\alpha)}{(\tau\alpha)_n} \right] * \overline{H_t} * N * \frac{A_c}{l}$$

$$f = 1.029Y - 0.065X - 0.245Y^2 + 0.0018X^2 + 0.0215Y^3, \quad F = \frac{\sum f_i L_i}{\sum L_i}$$

Appendix B

Comments on the results:

Figure 4.1 shows Benghazi North power Plant power output variation with ambient temperature for base load for both the Gas Turbine standalone and the Combined cycle .It is found that the Gas Turbine standalone output power decreases with the increase of the ambient temperature ,where the output dropped from 346.62 MW at 5 °C to 286.69MW at 37 °C with a reduction in the power output by 17.29 % .For the temperature range between 10 °C and 40 °C Fellah[38] reported a reduction percentage by 23.7 % and Ibrahim [9] stated that when the ambient temperature reaches 50 °C the gas turbine power output drop by 24 % . As can be seen from the plotted results in the same figure when the inlet air was cooled from 37 °C to 15 °C the Gas Turbine standalone performed better than the cycle without air cooling, where the power increased from 286.69 MW to 328.43 MW with increased power by 14.56 % .

Figure 4.1 also show that for the combined cycle(C.C) at base load as the ambient air temperature increase, the C.C power

output decreases, for instance the power reduced from 495.681 MW at 5 °C to 430.999 MW at 37 °C by 13.05 % with acceptable agreement with that recorded by aziza (12.34%). When the inlet air was cooled the C.C power output increased from 430.999 MW at 37 °C to 476.006 MW at 15 °C with power output increasing by 10.44 % . Q.M. Jaber [39] reported that about 30 % increase in the power output when supplying the inlet air to 10 °C. Ana Paula [40] concluded that the power output gain was 8.4 % to 12.7 % with use of inlet air cooling ,also Nasser[41] recommended the use of single effect water lithium bromide absorption chiller system for gas turbine intake air cooling to 10 °C at 40 °C leads to increase the power output by 10 %.

The results depicted in the figure 4.2 show the effect of ambient air temperature on the gas turbine standalone and the combined cycle . As can be seen from the figure the gas turbine standalone thermal efficiency reduced from 37.15 % at 5 °C to 33.1 % at 50 °C by reduction of 10.9 % (i.e thermal efficiency drops by 0.242 % for each 1 °C ambient air temperature rise).The C.C thermal efficiency is also inversely affected by the ambient temperature rise, where it reduced from 53.13 % at 5 °C to 51.72 % at 37 °C by reduction of 2.65 % which is in a good agreement with what resulted by aziza (2.5 %) . When the inlet air

is cooled to the ISO condition (15 °C ,RH 60 %),both efficiencies of the gas turbine standalone and the C.C where improved and increased from 34.4 % and 51.72 % at 37 °C to 36.41 % and 52.77 % by increasing percentage of 5.84% and 2.03% (i.e.0.265 % and 0.092 % for each lowered 1 °C ambient air temperature) .

The graphs plotted in figure 4.3 show that there has been a marked increase in specific fuel consumption with the increase of ambient temperature in Benghazi North power plant for both the Gas Turbine standalone and the C.C ,where the specific fuel consumption increased from 207.346 g/kWh and 144.993 g/kWh at 5 °C to 232.679 g/kWh and 149.821 g/kWh at 50 °C ,by increasing of 12.22 % and 3.33 % respectively .As can be seen from the figure when the inlet air was cooled from 37 °C to the ISO conditions ,the specific fuel consumption decreased for both Gas Turbine standalone and the combined cycle from 223.919 g/kWh and 148.945 g/kWh to 211.552 g/kWh and 145.965 g/kWh by reduction of 5.523 % and 2 % respectively.

Figures 4.4 and 4.5 shows the effect of condenser inlet cooling water temperature variations on the power output and thermal efficiency of the combined cycle power plant with cooled intake air from 37 °C , $\phi = 60\%$ to 15 °C , $\phi = 60\%$, It can be seen that the power output and thermal efficiency increased

from 476.006 Mw and 52.77 % at condenser inlet cooling water tw_1 of 27°C to 491.776 Mw and 54.52% at condenser inlet cooling water temperature of 8°C with increasing percentage of 3.313% and 3.316% respectively .

Figures 4.6 and 4 .7 shows the combined cycle power output and thermal efficiency without Intake air cooling as a function of condenser inlet cooling water. The result shows that the combined cycle power and thermal efficiency decreases with increase in CICWT (tw_1). Decreasing tw_1 will result to higher power output for the same mass flow rate and fuel input into gas turbine unit resulting in higher work output of the steam turbine. The power output and thermal efficiency increased from 430.999 Mw and 51.72 % at the condenser inlet cooling water $tw_1= 27$ °C to 446.798 Mw and 53.61 % at the condenser inlet cooling water of $tw_1 = 8$ °C with increasing percentage of 3.666 % and 3.654 % respectively and an additional power of 15.78 MW was achieved about 0.83 MW for each 1°C condenser inlet cooling water temperature drop. Alus[12] in his study found an improvement in the power output and thermal efficiency by 3.336 % and 3.664 % .

From figures 4.8 as the condenser inlet cooling water temperature increase the combined cycle specific fuel consumption increased from 141.284 g/ kwh at $tw_1= 8$ °C to 145.965 g/kwh at

$tw1=27\text{ }^{\circ}\text{C}$ by increasing percentage of 3.313%, so it should be noted that to enhance the plant output and efficiency there is a need to lower the vacuum pressure in the condenser through the cooling of the condenser inlet cooling water .

The results depicted in figure 4.9 show that as the ambient temperature rises the rate of CO_2 emission per kWh increase, for instance the rate of CO_2 emission increased for both the Gas Turbine standalone and the combined cycle from 551.82g CO_2/kWh and 381.5 g CO_2/kWh at $5\text{ }^{\circ}\text{C}$ to 619.34 g CO_2/kWh and 395.44 g CO_2 /kWh at $50\text{ }^{\circ}\text{C}$ by increasing of 12.24% and 3.63 % respectively, and by cooling the inlet air from $37\text{ }^{\circ}\text{C}$ to $15\text{ }^{\circ}\text{C}$,the rate of CO_2 emission declined from 595.93 g CO_2/kWh and 391.37 g CO_2/kWh to 563.03 g CO_2/kWh and 384.62 g CO_2/kWh by reduction of 5.52 % and 1.72 %.

The results depicted in figure 4.10 show that as the CICWT ($tw1$) rises the rate of CO_2 emission per kWh increase, for instance the rate of CO_2 emission increased for the combined cycle from 388.5 g CO_2/kWh at $tw1 = 8\text{ }^{\circ}\text{C}$ to 401.4 g CO_2/kWh at $tw1 = 27\text{ }^{\circ}\text{C}$ by increasing of 3.32 % and consequently the CO_2 emission treatment cost will be effected

Figure 4.11 shows predicted rates of heat gain and heat loss from the solar field for August 16, using calculations for heat

transfer to HTF, and receiver heat loss. The figure shows the energy that is absorbed by the receiver tubes (Q_{absorbed}), as well as the receiver and piping heat losses (Receiver heat loss and piping heat loss, respectively) and the energy that is absorbed by the heat transfer fluid after thermal losses from the receiver and piping losses have been accounted for (Q_{retained}). All energy rates shown in the figure are normalized on a per unit solar field aperture area basis, so their units are $[\text{W}/\text{m}^2]$. As can be noted from the figure the total predicted DNI on the solar field was $127,508.8 \text{ Wh}/\text{m}^2$, the energy absorbed ($Q_{\text{absorbed}} = 84,020.59 \text{ Wh}/\text{m}^2$) which represents 65.89% of DNI, the Receiver heat loss was $5,307.028 \text{ Wh}/\text{m}^2$ and it represents 4.16% of DNI, and piping heat loss was $65.779 \text{ Wh}/\text{m}^2$ which represents 0.052% of DNI, while (Q_{retained}) was $78,648.04 \text{ Wh}/\text{m}^2$ and it represents 61.68% of DNI after thermal losses subtracted from (Q_{absorbed}).

Figure 4.12 shows a linear increasing of the receiver heat losses as the bulk temperature of the fluid increases due to the created difference between the fluid temperature and the surrounding ambient air. This linear increasing in the range of the fluid bulk temperature between 50°C and 100°C is in good agreement compared with Patnode.

Figure 4.13 Shows the variation of solar field efficiency under load and no heat addition to the storage tank with time where the average value of solar field efficiency is 0.477.

Figure 4.14 shows effect of direct normal insolation change on the energy absorbed. As seen from the figure when the DNI was 927.3W/m² the total amount of absorbed energy(Q_{absorbed}) through all of operation hours was 85100.5W/m² and the maximum value of Q_{absorbed} reached to a value of 597 W/m² while these values decreased to 36708.9W/m²and 258W/m² at DNI equals to 400 W/m² by reduction of 56.9%.

Figures 4.15 and 4.16 show clear effect of direct normal insolation variation on both of receiver heat loss and the solar field piping heat loss, where the total receiver heat losses increased from 3,096W/m²at insolation of 400 W/m² for all operation hours to 5,542W/m² at insolation of 927.3 W/m² by increasing percentage of 79%,while the solar field piping heat losses also increased from 36.79 W/m² at DNI 400 W/m² to 71.2 W/m² at DNI 927.3 W/m² by increasing percentage of 93.5%. This increase in the heat losses will effect inversely on the amount of energy absorbed by the receiver and consequently on the solar field efficiency.

Figure 4.17 shows the effect of direct normal insolation variations on the collected energy by the receiver. Noted from the

figure as the insolation increases the collected energy increase also the receiver heat losses increases too, which effect on the solar field efficiency. When the DNI was 400W/m² the total amount of absorbed energy by receiver(Q_{collected}) was 33,576W/m² and its maximum value is 238.8W/m² and when DNI increased to 927.3 W/m² the total amount of absorbed energy by receiver(Q_{collected}) increased to 79,488W/m² and its maximum value reached to560.5 W/m² with increasing percentage of 136.7% and134.7% respectively, ref.[42]recorded 150% enhancement in energy collected between tow values of DNI 510W/m² and 700 W/m². This shows the high effect of DNI on heat gain.

Figure 4.18 Illustrates how changes of the mass flow rate affect the average collector efficiency. The figure shows that the efficiency varies linearly with the mass flow rate and this in agreement with Patel and Hansson[153]. When the mass flow rate was 2 kg/s with an average efficiency of 21.24% and when the mass flow rate increased to 6kg/s the average efficiency reached a value of 0.566% with an increasing percentage of 33.3%.This can be explained by the increased pressure that arises in the tubes of the collector when increasing the flow rate. The heat transfer fluid conducts heat when it comes in contact with the walls of the collector pipes. When increasing the mass flow rate, more water will interact with the walls of the pipes due to turbulent flow.

Higher flow rate will also contribute to the transfer fluid passing the collector pipes more frequently, causing the water to heat faster. Therefore the mass flow has a large impact on the collector efficiency.

Figure 4.19 shows the effect of wind velocity on solar field efficiency. As seen from the figure when the wind velocity was 2m/s the value of the average efficiency was 46.48%, and as the wind velocity increases the average efficiency decreased where it decline to 42.56% at wind velocity of 6 m/s by reduction of 8.4%. The results depicted in figure 4.20 show how the receiver heat losses directly increases with the increase of wind velocity where it rises from 25.1 W/m² at 2m/s to 35.5 W/m² at 6m/s with increasing percentage of 41.43% which strongly affects the solar field efficiency as can be seen from fig.4.49.

Figure 4.21 represents the daily load curve of the Libyan eastern network, the actual total generated power in august 16 through 24 hours was 27,491MWh and by using cooling technology the generated power increased to 27,875 MWh with an additional power of 16 MW in each hour of 24 operation hours and the curve load enhanced by 1.45% as seen in the figure, which contributes in increasing the maximum available power and help to cover any shortage in the national grid and save money in importing energy from neighboring countries.

A detailed analysis has been carried out on the power enhancement of the capacity of Benghazi (North) power plant considered gas-turbine with the selected 9.1193 MW cooling capacity for the design compressor inlet air temperature of 15 °C and the steam turbine condenser inlet cooling water. The results are plotted in fig. 4.22 which show the effect of the cooling technology on the monthly electrical energy production enhancement .

Fig 4.23 shows contribution of solar system integrated with HRSG waste heat covering annual cooling load of Benghazi North Power Plant intake air

Where the storage tank temperature should not be less than 80 °C. When the HRSG downstream exhaust gases used as heat source, the temperature T_{st} unstable and went down less than 80 °C because of no enough heat capacity in the HRSG downstream exhaust gases $C_p=0.662$ kJ/kg, $t=102$ °C and 96.6°C. When the heat added in the tank by solar energy only during the sunny hours, T_{st} was less than 80°C during the first 9 hours then it raised to 80°C this is need an additional auxiliary heat source to make up any temperature drop, while when only fuel fired as a heat source in the tank, the storage tank temperature T_{st} maintained at 80°C as seen in figure 4.52 which help to drive the cooling unit easily but the continuous fuel firing costs more money and the pollutants emitted makes this scenario unfavourable. The integration of solar energy

with the HRSG downstream exhaust gases as seen from the figure makes this mode or scenario more reliable and effective heat source in the storage tank and Tst raised above the operation temperature 83.25°C.